Human Laminin-111 and Laminin-211 protein therapy prevents muscle disease progression in an immune deficient mouse model of LAMA2-CMD

Pamela Barraza-Flores
University of Nevada Reno

Hailey J. Hermann
University of Nevada Reno

Christina R. Bates
University of Nevada Reno

Tyler G. Allen
University of Nevada Reno

Timothy T. Grunert
University of Nevada Reno

Dean J. Burkin (✉ dburkin@med.unr.edu)
University of Nevada Reno   https://orcid.org/0000-0001-9228-5258

Research

Abstract

Background

Laminin-α2 related Congenital Muscular dystrophy (LAMA2-CMD) is a devastating genetic disease caused by mutations in the LAMA2 gene. These mutations result in progressive muscle wasting and inflammation leading to delayed milestones, and reduced lifespan in affected patients. There is currently no cure or treatment for LAMA2-CMD. Preclinical studies have demonstrated that mouse Laminin-111 can serve as an effective protein replacement therapy in a mouse model of LAMA2-CMD.

Methods

In this study, we generated a novel immunocompromised dy W mouse model of LAMA2-CMD to study the role the immune system plays in muscle disease progression. We used this immune deficient dy W mouse model to test the therapeutic benefits of recombinant human laminin-111 and laminin-211 protein therapy on Laminin-α2 deficient muscle disease progression.

Results

We show that immune deficient Laminin-α2 null mice demonstrate subtle differences in muscle regeneration compared to immune competent animals during early disease stages, but overall exhibit a comparable muscle disease progression. We found human laminin-111 and laminin-211 could serve as effective protein replacement strategies with mice showing improvements in muscle pathology and function. We observed that human laminin-111 and laminin-211 exhibit differences on satellite and myoblast cell populations and differentially affect muscle repair.

Conclusions

This study describes the generation of a novel immune deficient mouse model that allows investigation of the role the immune system plays in LAMA2-CMD. This model can be used to assess the therapeutic potential of heterologous therapies that would illicit an immune response. Using this model, we show that recombinant human Laminin-111 can serve as effective protein replacement therapy for the treatment of LAMA2-CMD.

Introduction

Laminin-α2 related Congenital Muscular Dystrophy (LAMA2-CMD) also known as known as Merosin Deficient Congenital Muscular Dystrophy type 1A (MDC1A) is a severe genetic disease with an incidence estimated at 1−9/100,000 people and representing 10−30% of all congenital dystrophies [1−3]. LAMA2-CMD patients present with neonatal hypotonia, muscle wasting resulting in wheelchair confinement and requiring respiratory support at a young age. There is currently no effective cure or treatment for LAMA2-CMD [4] and patients often die from respiratory insufficiency as early as during their first decade of life [5].

Although mutations can cause partial or reduced expression of LAMA2, mutations that result in a complete absence of the Laminin-α2 protein chain cause the most severe muscle disease and clinical outcomes in patients. Laminin-α2 is a critical component of the Laminin heterotrimer, which along with Laminin-β1 or β2 and laminin-γ1 form the structural glycoproteins laminin−211 and laminin−221 in skeletal muscle. Laminin−211 and 221 polymerize with each other and interact with nidogen and collagen-IV to form the muscle basal lamina. Laminin−211 and Laminin−221 bind to muscle cell surface through the α7β1 integrin and α-dystroglycan of the dystrophin glycoprotein complex via their globular C-terminal domains. This interaction anchors muscle cells to the basal lamina and regulates mechanotransduction and cell signaling [6,7]. Loss of these Laminin−211 and Laminin−221 in LAMA2-CMD disrupts these molecular interactions and results in reduced muscle strength, failed muscle regeneration, inflammation and fibrosis [1,4,5].

Severe inflammation is a hallmark of LAMA2-CMD and muscle biopsies from mouse and LAMA2-CMD patients exhibit immune cell infiltration especially during early stages of the disease. However, in contrast with other muscular dystrophies, inflammatory infiltrate is decreased during later stages of LAMA2-CMD muscle disease progression and its role in LAMA2-CMD muscle disease remains unclear [5,8,9].

In this study, to determine the role the immune response plays in LAMA2-CMD muscle disease, we produced a novel immune deficient Lama2-null mouse in on the dy^W background. This novel mouse line, which we designated NODScid dy^W, lacks laminin-α2 and functional B and T-immune cells. This new model was compared to the immune competent dy^W mouse model to assess the impact the loss of the immune response plays in LAMA2-CMD muscle disease. The immune deficient NODScid dy^W mouse model showed reduced levels of basal regenerating myofibers compared to dy^W animals. At later stages, there were no differences between immune deficient and immune competent mice in terms of disease progression. These results indicate the immune response contributes to initial muscle disease in LAMA2-CMD, but that other non-immune related mechanisms contribute to long-term muscle disease progression.

Laminin−111 is a form of Laminin that is structurally and functionally similar to laminin−211 and 221 and has been shown to rescue mouse models of LAMA2-CMD [10−13]. We next determined the efficacy of recombinant human laminin−111 (HsLAM−111) and laminin−211 (HsLAM−211) protein therapies to prevent muscle disease progression using this immune deficient dy^W mice model. Our results show that treatment with HsLAM−111 and HsLAM−211 improved muscle function and pathology, but results show HsLAM−111 and HsLAM−211 had different efficacies on muscle regeneration. Together these studies indicate a role for the adaptive immune response in LAMA2-CMD and support the idea of Laminin protein replacement therapies as a treatment option for LAMA2-CMD.

Results

The NODScid dy^W mouse is immuno-deficient and lacks Laminin-α2 protein

To produce an immunodeficient mouse model of LAMA2-CMD, NODScid mice were bred with dy$^{W+/-}$ animals. Along with the test group NODScid dy^W, we also generated wild type, NODScid and dy^W control groups. Muscles from wild type, NODScid, dy^W, and NODScid dy^W were harvested at 6-weeks of age and immunofluorescence used to detect the Laminin-α2 chain. While strong signal for Laminin-α2 immunofluorescence was observed in wild-type muscle, little signal was detected in dy^W and NODScid dy^W muscle (Figure 1A). These results confirmed NODScid dy^W lacked Laminin-α2 in skeletal muscle.

To determine if NODScid dy^W lacked an adaptive immune system, we next isolated serum from 6-week old mice and performed an ELISA to detect serum immunoglobulin G (IgGs). Our results show that while wild type and dy^W mice had high levels of IgG in serum, NODScid and the NODScid dy^W serum had no detectable IgGs (Figure 1B). These results confirmed that NODScid dy^W animals lack functional B-cells and are unable to produce immunoglobulin.

Next, we used fluorescence-activated-cell sorting (FACS) to quantify circulating levels of T and B cells in blood. Hematopoietic cells (CD45$^+$) from sera of wild type and NODScid dy^W were co-labeled with T-cell marker (CD3ε$^+$) and B-cell marker (CD19$^+$) (Figure 1C). Results showed that in wild type 31.6% of CD45$^+$ cells were CD3ε$^+$ and 38.4% were CD19$^+$. In NODScid dy^W, 0.88% were CD3ε$^+$ and 1.08% were CD19$^+$. These results show that NODScid dy^W mice lack functional T- and B-cells and therefore lack an adaptive immune response.

Muscular dystrophy in NODScid dy^W is comparable to the dy^W mouse model of LAMA2-CMD

We next performed a survival study using wild type, NODScid, dy^W and NODScid dy^W experimental groups. We observed that neither the female nor the male NODScid dy^W groups had a significant increase in lifespan compared to dy^W (Figure 2A and 2B). Male and female NODScid showed reduced lifespan compared to wild-type mice, consistent with reports on radio-sensitivity induced lymphomas [14]. Symptoms of lymphomas were not observed in the NODScid dy^W mouse. Weekly body mass showed no significant gender differences between NODScid dy^W and dy^W animals (Figure 2C and 2D). These data indicate growth and survival were similar between immune competent and immune deficient dy^W animals.

To determine if loss of the immune system affected muscle strength in dy^W mice, a forelimb grip-strength test was performed at 6 weeks of age and normalized to body weight as previously described [15]. As expected, 6-week old wild type and NODScid mice exhibited an average of 3-fold increase in muscle grip

strength compared to dystrophic dy^W and NODScid dy^W groups. Interestingly, 6-week-old NODScid dy^W males showed a 1.4-fold increase in grip strength compared to dy^W males (Figure 3A; N = 6 and 7, respectively, p-value <0.0001). In contrast, dy^W and NODScid dy^W females did not show any differences (Figure 3B). These results suggest that the immune response in dystrophic muscle contributes to the lower grip strength observed in male dy^W animals.

To determine if the immune response in dystrophic muscle contributed to fibrosis observed in LAMA2-CMD, we used Sirius red to stain sections from TA muscles (Supplemental Figure 1A) and quantified levels of hydroxyproline as previously described [16] (Supplemental Figure 1B, C) in quadriceps of all groups. Sirius Red staining indicated more fibrosis in TA muscle sections from dy^W and NODScid dy^W mice compared to wild type and NODScid muscle. This was confirmed and quantified using a hydroxyproline (HOP) assay. Wild-type and NODScid muscle had approximately 1.5-fold less HOP in their TA muscles compared to dystrophic dy^W and NODScid dy^W mice. There was no difference in HOP levels between males and females in the dy^W and NODScid dy^W experimental groups. These results indicate the immune response did not play a major role in the development of TA muscle fibrosis in 6-week-old dy^W mice.

To assess for the presence of other inflammatory cells, we used immunofluorescence to detect the three major myeloidal cell infiltrates: Eosinophils, macrophages (CD11B) (Supplemental Figure 2) and neutrophils (LysC) (Supplemental Figure 3) associated with muscular dystrophy [8,17]. Our results showed presence of innate immune infiltrates in NODScid dyW and dyW muscle, suggesting genetic ablation of the adaptive response through NODScid immune suppression did not affect greatly the innate immune infiltration in these animals.

Immune deficient dyW mice exhibit decreased muscle repair

Laminin-α2 deficiency leads to failed muscle regeneration and early apoptosis of regenerating myofibers [1,18–20]. To assess differences in levels of ongoing regeneration in the NODScid dy^W, we quantified embryonic Myosin Heavy Chain (eMHC), a marker for muscle regeneration, in TA sections (Figure 4A). When compared to dy^W, we found that both male and female NODScid dy^W groups showed a decrease in eMHC positive fibers: from 8.77±0.81% in dy^W and 5.86±0.535% in NODScid dy^W males (N = 7, 5 respectively, p-value 0.01) and 6.09±0.50% in dy^W and 4.31±0.40% in NODScid dy^W females (N = 5, 4 respectively, p-value 0.02) (Figure 4B and 4C).

Feret minimal diameters were used to measure myofiber size. Male myofibers showed a shift towards increased in myofiber diameter, from a mean of 30.11μm in dy^W to 34.81μm in NODScid dy^W (N = 4, 5 respectively, p-value <0.0001). Female myofibers, however, did not show a shift with a mean of 34.00μm in dy^W to 34.98μm in NODScid dy^W (N = 5, p-value 0.114) (Figure 4D and 4E). This data suggests that

NODScid dyW muscle exhibits a lower level of basal muscle damage compared to dy^W. This may indicate that suppression of adaptive immunity in Laminin-α2 deficient skeletal muscle results in decreased muscle damage that results in muscle hypertrophy in male animals.

Human Laminin−111 and Laminin−211 protein therapy increase muscle repair in NODScid dyW

Previous research has shown that treatment with natural Englebreth-Holm-Swam (EHS) murine sarcoma derived Laminin−111 enhances muscle regeneration and prevents myopathy of mouse models of LAMA2-CMD and Duchenne Muscular Dystrophy (DMD) [10,11,16,21−23]. To test whether human Laminin−111 has the same effect, we treated NODScid dy^W mice with HsLAM−111. We also used HsLAM−211 to investigate if it could completely substitute for the loss of Laminin-α2 in LAMA2-CMD.

Female NODScid dy^W mice were treated from 2 to 6 weeks of age with weekly retro-orbital injections of 1 mg/kg HsLAM−111, HsLAM−211 or vehicle (Figure 5A). This dose was 10-fold lower than previous studies [13,16,22] due to production availability of HsLAM−111 and HsLAM−211 (BioLamina, Sundeberg, Sweden) at 0.1 mg/ml compared to EHS Laminin−111 (Thermo Fisher, Waltham MA) at 1 mg/ml. At 6 weeks of age, mice were humanely euthanized, and TA, gastrocnemius, quadriceps and triceps were harvested.

TA muscle sections were tested for presence of laminin protein using immunofluorescence. Two antibodies directed against the carboxyl-terminal and rod domains of human Laminin-β1 chain were used for immunofluorescence using muscle from vehicle and HsLAM−111 treated groups. Supplemental Fig.4A shows positive immunofluorescence for both domains in HsLAM−111 compared to PBS treated groups. Additionally, we used western analysis to show these antibodies are specific for the human isoform of Laminin−111 (Supplemental Fig. 4B). We were unable to detect HsLAM−211 as antibodies against laminin−2 were not specific for the human isoform and the dy^W mouse model expresses a low level of truncated laminin−2 protein.

TA cryosections were subjected to immunofluorescence for eMHC-positive fibers. We found that treatment with both HsLAM−111 and HsLAM−211 resulted in a ~1.7-fold increase in levels of eMHC-positive fibers in laminin treated muscle compared to vehicle treatment (Figure 5B). Where PBS treated mice showed 3.03± 0.48% eMHC-positive fibers, HsLAM−111 treatment resulted in a 5.192± 19% (N = 7, 5 respectively, p-value <0.05) and HsLAM−211 treatment in a 5.37±0.23% (N = 7, 6; p-value of 0.004).

We next measured myofiber size using Feret's minimal diameters, and observed a change in the mean from 23.68μm in PBS treated animals, 18.09μm for HsLAM−111 treatment and 20.76μm in HsLAM−211 treatment (N = 7, 5, 7 respectively; p-value < 0.0001). We observed a decrease in the standard deviations of myofiber size in laminin treated muscles (SD) from 8.35μm in PBS to 7.6μm HsLAM−111 and 7.17μm in HsLAM−211, indicating laminin treatment promoted a reduction in myofiber size variability (Figure 5C).

Centrally located nuclei (CLNs) fibers were also quantified as a measure of ongoing repair (data not shown), but showed no differences between vehicle and treatment groups.

Together these data suggest that treatment with HsLAM−111 and HsLAM−211 increased muscle regeneration and reduced fiber diameter variability.

Human Laminin−111 and Laminin−211 differentially affected myogenic cells in Laminin-α2 deficient muscle

To test the effect of HsLAM−111 and HsLAM−211 on muscle repair, we next quantified satellite and myogenic cells in TA muscle. For satellite cells we conducted immunofluorescence for the Paired-box transcription factor 7 (Pax7) and counted the number of Pax7 positive cells located adjacent to the myofiber under the basal lamina (Figure 6A). Treatment with HsLAM−111 resulted in a significant decrease in the numbers of satellite cells from 2.06±0.14 cells per frame in PBS to 1.38±0.19 Pax7 positive cells (N = 8, 6 respectively, p-value <0.05). In contrast, we observed a significant increase in satellite cells in muscle with HsLAM−211 treatment to 2.70±0.17 satellite cells compared to HsLAM−111 or PBS treatments (N = 6, p-value <0.0001 and p<0.05 respectively) (Figure 6B).

To determine if recombinant human Laminin treatment affected myogenic differentiation, we counted myogenin positive cells (Figure 6C). Our results showed no significant decrease of myogenin-positive cells from 8.1±0.79 cells per area in PBS treated animals to 7.56±0.89 in HsLAM−111 treated mice. However, we did see a significant decrease to 4.78±0.95 cells per frame in HsLAM−211 treated mice (N = 6, 7 respectively, p-value of 0.01) (Figure 6D).

Together these results may suggest that Laminin−111 and Laminin−211 isoforms have an effect on muscle repair in Laminin-α2 null muscle, while differentially promoting myogenic cell differentiation.

Human Laminin−111 treatment improves the activity of LAMA2-CMD mice

Previous studies have shown that treatment with EHS derived mouse laminin−111 improves muscle function in the dy^W mouse model. To test the human isoform of this biologic, NODScid dy^W mice were treated with HsLAM−111, HsLAM−211 or PBS for several weeks. Mice were then subjected to a computer controlled activity assay as previously described [10] (Figure 7A). Results showed a significant increase in distance traveled from a mean of 3394±479cm in PBS treated mice to 5386±281.7cm in HsLAM−111 treatment (Figure 7B) (N = 7, 7 respectively; p-value <0.05), but no increase in HsLAM−211 treated mice with 3211±724.9cm. Resting time showed no significant decrease from a mean of 236.8±54.4 seconds in PBS to 109.8±12.38 seconds in HsLAM−111 and 238.6±41.66 in HsLAM−211 treatment groups (Figure 7C). Finally, HsLAM−111 treated mice showed a significant increase in vertical breaks from 11.2±9.5 in PBS to 50±11.3 in HsLAM−111 treated animals, indicative of increased use of hindlimbs during the

assay (Figure 7D) (N = 7, 7; p-value 0.0005). Grip strength was also performed with no significant differences between treatment groups (Supplemental Fig, 5) (N = 6). These data indicate treatment with recombinant human laminin−111 improves mobility of Laminin-α2 deficient mice.

Discussion

Mouse laminin−111 has previously shown to be an effective protein based therapy in the dy[W] mouse model of LAMA2-CMD [10,13]. Although mouse and human laminin−111 have a high degree of homology, there are ~30% differences in the amino acid sequence in addition to differences in glycosylation patterns. For this reason, treatment using the recombinant HsLAM−111 is likely to generate an immune response in mice that could complicate interpretation of the efficacy of the human biologic. To investigate if recombinant human laminin−111 could prevent disease progression, we generated an immune deficient dy[W] mouse model of Laminin-α2 related congenital muscular dystrophy (LAMA2-CMD). We demonstrate that this mouse model has disrupted expression of Laminin-α2 protein and an ablated adaptive immune system. Histological and physiological characterization of this new mouse model shows severe muscle disease progression comparable to the established dy[W] model of LAMA2-CMD.

The NOD Scid mouse has been shown to present multiple defects in innate and adaptive immunity and has been used extensively in xeno engraftment studies [24,25]. Reduced Natural Killer (NK) cell activity, decrease in functionally mature macrophages and ablation of functional lymphoid T and B cells, are the main immune deficiencies reported in NODScid mice [14,26]. The generation of a Laminin- α2 deficient mouse that is also NODScid allows for a study of the role of the innate and adaptive immunity plays in LAMA2-CMD disease progression.

A case study of several Laminin-α2 deficient patients reported high levels of T and B-cell infiltration in skeletal muscle at an early age, but decreased inflammatory infiltration at later stages of the disease [27]. This suggests that in contrast with other muscular dystrophies, the immune system in LAMA2-CMD may not play a major role in later disease progression [8]. The immune response may, however, be important during neonatal stages and may exacerbate muscle disease progression. Our studies demonstrate there were no changes in the survival or weight of immunocompromised and immunocompetent dy[W] animals. Lack of improved grip strength and hypertrophy in females as opposed to males is consistent with reports of more severe myopathy in females vs males in other LAMA2-CMD mouse models [28]. Another possible explanation may be sex-dependent differences in immune infiltration or timing between males and female during disease stages. The observed differences between male and female myopathy and inflammation in LAMA2-CMD remains to be further explored.

Loss of immune function did result in reduced muscle regeneration in NODScid dy[W] mice as indicated with eMHC expression. The reduced levels of muscle regeneration and larger myofibers found in the NODScid dy[W] mouse indicate of a role of an active immune response in promoting muscle regeneration in LAMA2-CMD.

Together these results suggest the NODScid dy^W is a viable immuno compromised model for LAMA2-CMD, that while presenting reduced levels of basal muscle regeneration, disease progression is comparable to the established dy^W model and similar to LAMA2-CMD patients. This immune deficient mouse model of LAMA2-CMD might be beneficial to investigate the role the immune system plays in LAMA2-CMD, or investigate the efficacy of human cell-based or human biologics for the treatment of LAMA2-CMD.

Using this novel mouse model of LAMA2-CMD, we next tested the efficacy of recombinant human laminin−111 and laminin−211 to act as protein substitution therapies and prevent muscle disease progression for LAMA2-CMD. Previous research has shown treatment with EHS murine laminin−111 can promote muscle regeneration and prevent muscular disease in mouse models of muscular dystrophy. To our knowledge, this is the first study to investigate the therapeutic potential of recombinant human laminin−111 and laminin−211 in a muscular dystrophy disease model.

Our results showed that HsLAM−111 and HsLAM−211 increased the regenerative capacity of muscle, but that the mechanism of action of these laminin isoforms on satellite cells and myoblast were different. Laminin−111 promoted muscle repair at the expense of satellite cells, while laminin−211 preserved satellite cell populations in skeletal muscle. This could indicate that HsLAM−111 treatment induces satellite cell activation, which may explain the increase in eMHC positive regenerative fibers observed in this treatment groups. However, continuous long-term treatment with HsLAM−111 could deplete satellite cells. On the other hand, treatment with HsLAM−211 increased satellite cells and decreased myogenin-positive cells suggesting this Laminin isoform could support the satellite cell niche in a way that preserves the satellite cell population. It is also possible that the local concentrations of laminin isoforms are critical for proliferation vs differentiation of myoblasts. Finally, we show that treatment with HsLAM−111 improved the activity of Laminin-α2 null mice.

This short-term study of HsLAM−111 and HsLAM−211 in skeletal muscle provided preliminary data for the treatment of LAMA2-CMD. A long-term treatment using these biologicals is necessary to assess improvements in survival, immune infiltration and fibrosis. Additionally, it is important to explore the long-term effect on satellite cell depletion and renewal, as well as the potential for the combination of HsLAM−111 and HsLAM−211 therapies.

To our knowledge, this is the first report using a Laminin-α2 deficient mouse model to investigates the role that the immune system plays in LAMA2-CMD. In addition, this is the first report using an immune deficient preclinical model to explore the short-term efficacy of recombinant human Laminin−111 and Laminin−211 on LAMA2-CMD disease progression. Limitations of this approach include producing enough purified HsLAM−111 to treat LAMA2-CMD patients, potential immune responses to glycosylation differences between recombinant and native human laminin isoforms, and the effects of long-term systemic treatment with HsLAM−111 protein.

Materials And Methods

Generation of immune deficient NODScid dyW mice

All animal studies were performed under an approved animal protocol (#00404) reviewed by the Institutional Animal Care and Use Committee (IACUC) at the University of Nevada, Reno. To generate immune deficient dy^W mice, female $dy^{W\,(+/-)}$ mouse were mated to male NOD.CB17-$Prkdc^{SCID/}$Jfrom Jackson Laboratories. Offspring was genotyped for LacZ gene inserted in dy^W and the NOD (Non-Obese Diabetic) gene using PCR. The Scid gene was genotyped using qPCR using primers recommended by Jackson Laboratories. $NOD^{(+/-)}$ $Scid^{(+/-)}$ $dy^{W\,(+/-)}$ were mated to generate breeding pairs $NOD^{(-/-)}$ $Scid^{(-/-)}$ $dy^{W\,(+/-)}$ and $NOD^{(+/+)}$ $Scid^{(+/+)}$ $dy^{W\,(+/-)}$. Mattings of these mice generated wild-type, NODScid, dy^W and NODScid dy^W experimental groups.

Survival study

Wild-type, NODScid, dy^W and NODScid dy^W were aged until they reached morbidity or death. Morbidity was described as loss of 10% weight from week to week or severe kyphosis combined with hind-limb myopathy as defined within the approved IACUC protocol.

Generation and administration of recombinant Laminins

HsLAM−111 and HsLAM−211 were purchased from BioLamina (Sundberg, Sweden) where they are produced recombinantly at a stock concentration of 0.1mg/ml. HsLAM−111 and HsLAM−211 dialyzed overnight against PBS to remove preservatives. Mice were anesthetized using isoflurane and administered each treatment group (HsLAM−111, HsLAM−211 or PBS) weekly via retro-orbital injection.

Immunofluorescence

Muscles were harvested and embedded in 2:3 ratio of optimum cutting temperature (Fisher Scientific, Waltham, Massachusetts) and 30% sucrose medium prior to flash-freezing. Tissues were cryosectioned at 10μm thick and stained with Wheat Germ Agglutinin (WGA) (Vector Laboratories, Burlingame, California, 1:00) for 10 min. Slides were prepared using Vectashield mounting media with DAPI stain (Vector Laboratories, Burlingame, California). Immunostained sections were permeabilized using 0.2% Triton in PBS for 30 min before blocking, then primary antibodies anti-eMHC (Developmental Studies Hybridroma Bank (DSHB, Iowa City, Iowa, BF−45, 1:40), CD11B (Biolegend, San Diego, California, 1:800) LysC (Biolegend, San Diego, California, 1:800). Pax7 (Developmental Studies Hybridroma Bank (DSHB, Iowa City, Iowa, BF−45, 1:20) and Myogenin (Developmental Studies Hybridroma Bank (DSHB, Iowa City, Iowa, BF−45, 1:20) were incubated overnight. Antibodies against human Laminin−111-c-terminal and rod-terminal domains were used at a concentration of 1:20 without permeabilization. All stains were followed by secondary antibody incubation for 1h using FITC-anti mouse or FITC-anti rabbit antibodies (Jackson laboratories, Sacramento, California, 1:200), except for pre-labeled FITC-CD11b and FITC-LysC,

and lastly incubated for 10 min WGA stain (WGA−647 1:100). Slides were imaged using the Olympus Fluoview FV 1000 laser confocal microscope and analyzed using Image J-win32 software. Whole muscle cross-sections were imaged and used for quantification of fiber diameters and eMHC. 5 to 10 images were obtained at 40X magnification to quantify pax7 and myogenin positive cells. To measure fibrosis TA slides were stained with Sirius Red (Sigma-Aldrich, St. Louis, Missouri) as previously described (Van Ry, 2014). Images were captured using Axiovision 4.8 software.

Immunoblotting

At total of 1 mg of HsLam−111, HsLam−211 and EHS Laminin−111 (Thermo Scientific, Waltham, Massachusetts) proteins were separated in a NuPAGE 4 to 12% Bis-Tris gel (Thermo Scientific, Waltham, Massachusetts) and transferred onto a Nitrocellulose membrane. Laminin−111 C-terminal and rod-terminal domains were detected using home-made antibodies at a 1:100 concentration incubated overnight followed by 1-hour incubation with secondary antibody Alexa Fluor680 conjugated anti-rabbit (Invitrogen, Carlsbad, California). LI-COR imaging system was used to detect and image protein bands.

IgG detection

An Enzyme-linked immunoabsorbent assay (ELISA) was used to measure the relative levels of immunoglobulin (IgG) in mouse sera. Mouse sera was used to coat an Immulon 1B (Thermo Scientific, Waltham, Massachusetts) plate in triplicates overnight at 4C. After three 0.1%SDS washes, samples were incubated with mouse anti-IgG antibody at 1:200 dilution in 1% BSA overnight at 4C. After three more washes, samples were incubated with secondary antibody FITC-anti mouse (Jax labs, Bar Harbor, Maine). After the final wash, plate was read using Victor photospectrometer at 500 nm.

Fluorescence Activated Cell Sorting (FACS)

Blood samples were drawn from 6-week old mice into EDTA K3 coated tubes. One million cells were diluted with pre-labeled primary antibodies CD45 (1:800), CD19 (1:800), CD3ε (1:100) from BD biosciences (San Jose, California) and incubated for 30 minutes in the dark at room temperature. Cells were lysed using FACS lysis solution protocol (BD Biosciences Cat.no 349202) and washed in 0.5% Fetal Bovine Serum in PBS. Cells were quantified using the BD LSR II SORP cell analyzer and data was analyzed using FlowJo software.

Statistics

GraphPad Prism software was used for statistical calculations. Student's t-test was used to compare means between two groups and one-way ANOVA was used to compare means between three or more

groups. All ANOVA calculations were followed by Bonferroni post-test. Means of experimental groups were considered statistically significant when p<0.05.

Abbreviations

ANOVA: Analysis of Variance

B-cells: Bursa of Fabricius cells

CD: Cluster of Differentiation

cm: centimeter

C-terminal: Carboxyl terminal domain

DSHB: Developmental Studies Hybridroma Bank

DMD: Duchenne Muscular Dystrophy

EHS: Englebreth-Holm-Swam

ELISA: Enzyme-linked immunoabsorbent assay

eMHC: Myosin Heavy Chain

FACS: Fluorescence Activated Cell Sorting

FITC: Fluorescein Isothiocyanate

HOP: hydroxyproline

HsLAM−111: Laminin−111

HsLAM−211: laminin−211

IACUC: Institutional Animal Care and Use Committee

LAMA2-CMD: Laminin-α2-related Congenital Muscular Dystrophy

IgG: Immunoglobulin G

kg: kilogram

Merosin Deficient Congenital Muscular Dystrophy type 1A (MDC1A)

mg: milligram

NOD: Non-Obese Diabetic

Pax7: Paired-box transcription factor 7

PBS: Phosphate Buffered Saline

PCR: Polymerase Chain Reaction

qPCR: quantitative Polymerase Chain Reaction

p-value: probability value

Scid: Severe Combined Immunodeficiency

TA: Tibialis Anterior muscle

T-cells: Thymus lymphocyte cells

WGA: Wheat Germ Agglutinin

μm: micrometer

Declarations

Ethics approval: All vertebrate animal studies described in this manuscript were performed under an animal protocol (#00404) approved by the University of Nevada, Reno IACUC.

Availability of data and material: Most of the data generated and analyzed during this study are included in the manuscript or supplemental data. Any data not included will be made available from the corresponding author upon request.

Competing interests: The University of Nevada, Reno, has a patent on the therapeutic use of laminin-111 and its derivatives. This patent has been licensed to Prothelia Inc., and the University of Nevada, Reno has a small equity share in this company.

Author contributions: P.B-F. and D.J.B conceptualization and study design; P.B-F. methodology, validation, formal analysis; P.B-F., H.J.H, C.R.B, T.G.A., T.T.G, investigation; D.J.B. resources; P.B-F., writing original draft, P.B-F., D.J.B. writing-review and editing; P.B-F visualization, supervision; P.B-F., D.J.B. project administration; D.J.B. funding acquisition.
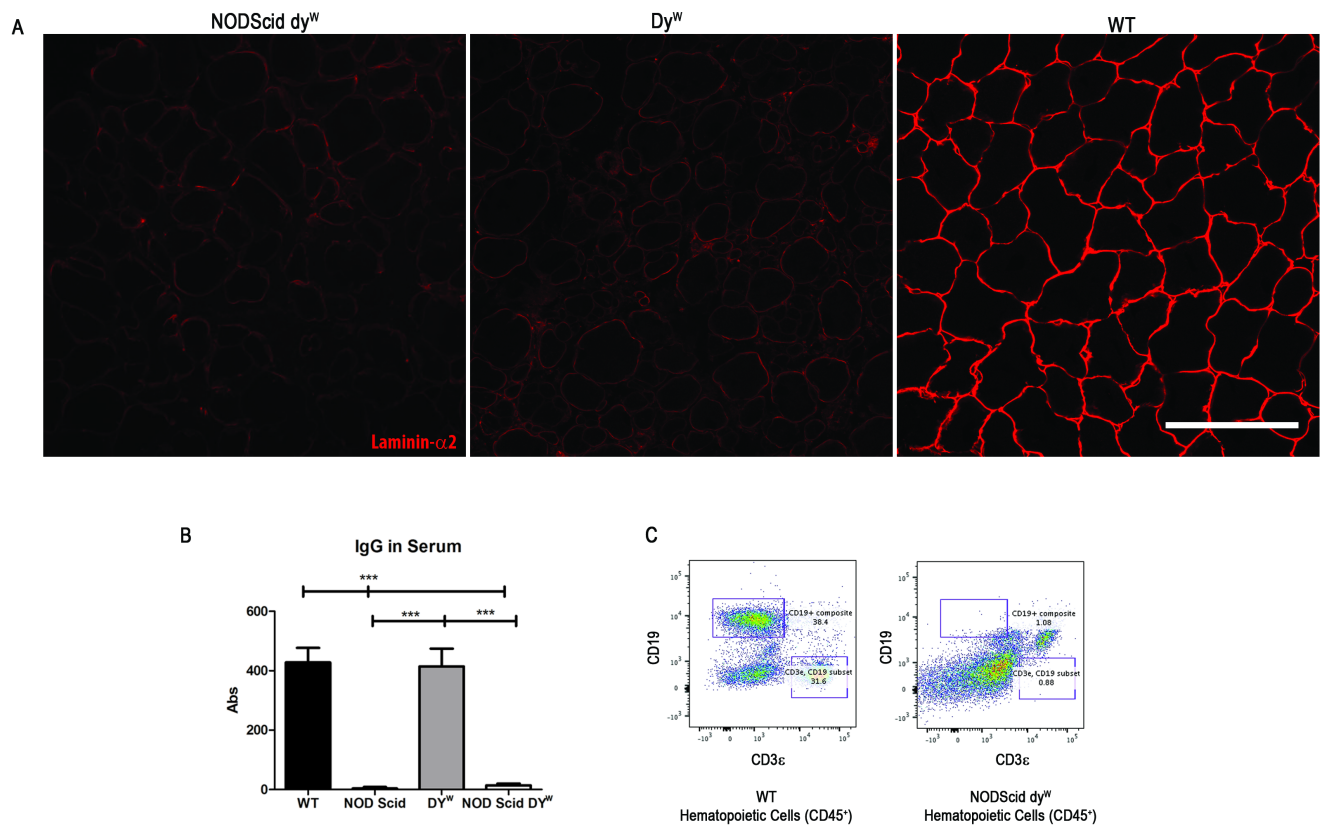
References

1. Mohassel P, Reghan Foley A, Bönnemann CG. Extracellular matrix-driven congenital muscular dystrophies [Internet]. Matrix Biol. 2018 [cited 2019 Apr 25]. p. 188–204. Available from: https://doi.org/10.1016/j.matbio.2018.06.005

2. Sframeli M, Sarkozy A, Bertoli M, Astrea G, Hudson J, Scoto M, et al. Congenital muscular dystrophies in the UK population: Clinical and molecular spectrum of a large cohort diagnosed over a 12-year period. Neuromuscul Disord. 2017;27:793–803.

3. N. D, M. T. Neuromuscular disorders in childhood: A descriptive epidemiological study from western Sweden. Neuromuscul Disord [Internet]. 2000;10:1–9. Available from: http://www.embase.com/search/results?subaction = viewrecord&from = export&id = L30006857%0Ahttp://dx.doi.org/10.1016/S0960–8966(99)00055–3

4. Nguyen Q, Lim KRQ, Yokota T. Current understanding and treatment of cardiac and skeletal muscle pathology in laminin-α2 chain-deficient congenital muscular dystrophy. Appl Clin Genet [Internet]. 2019 [cited 2019 Aug 22];Volume 12:113–30. Available from: http://doi.org/10.2147/TACG.S187481

5. Konkay K, Kannan M, Lingappa L, Uppin M, Challa S. Congenital muscular dystrophy with inflammation: Diagnostic considerations. Ann Indian Acad Neurol. 2016;19:356.

6. Patton BL. Laminins of the neuromuscular system [Internet]. Microsc. Res. Tech. 2000 [cited 2019 Mar 16]. p. 247–61. Available from: http://www.ncbi.nlm.nih.gov/pubmed/11054875

7. Patton BL, Miner JH, Chiu AY, Sanes JR. Distribution and function of laminins in the neuromuscular system of developing, adult, and mutant mice. J Cell Biol [Internet]. 1997 [cited 2019 Mar 16];139:1507–21. Available from: http://www.jcb.org

8. Tidball JG, Welc SS, Wehling-Henricks M. Immunobiology of Inherited Muscular Dystrophies. Compr Physiol [Internet]. 2018 [cited 2019 May 8];8:1313–56. Available from: https://onlinelibrary-wiley-com.unr.idm.oclc.org/doi/pdf/10.1002/cphy.c170052

9. Pegoraro E, Cianno B Di, Hoffman EP, Mancias P, Swerdlow SH, Raikow RB, et al. Congenital muscular dystrophy with primary laminin?2 (merosin) deficiency presenting as inflammatory myopathy. Ann Neurol [Internet]. 2005 [cited 2019 Jul 9];40:782–91. Available from: https://onlinelibrary-wiley-com.unr.idm.oclc.org/doi/pdf/10.1002/ana.410400515

10. Rooney JE, Knapp JR, Hodges BL, Wuebbles RD, Burkin DJ. Laminin–111 protein therapy reduces muscle pathology and improves viability of a mouse model of merosin-deficient congenital muscular dystrophy. Am J Pathol [Internet]. Elsevier Inc.; 2012;180:1593–602. Available from: http://dx.doi.org/10.1016/j.ajpath.2011.12.019

11. Gawlik KI, Harandi VM, Cheong RY, Petersén Å, Durbeej M. Laminin α1 reduces muscular dystrophy in dy2Jmice. Matrix Biol [Internet]. 2018 [cited 2018 Mar 26]; Available from: https://ac.els-cdn.com/S0945053X1830043X/1-s2.0-S0945053X1830043X-main.pdf?_tid = 2812fba9–3b9b–41d3-a452-ac0615da372b&acdnat = 1522110251_a4d296cbed8c6f6ced9d0014538bd588

12. Gawlik KI, Mayer U, Blomberg K, Sonnenberg A, Ekblom P, Durbeej M. Laminin α1 chain mediated reduction of laminin α2 chain deficient muscular dystrophy involves integrin α7β1 and dystroglycan. FEBS Lett [Internet]. 2006 [cited 2019 Aug 15];580:1759–65. Available from: https://febs-onlinelibrary-wiley-com.unr.idm.oclc.org/doi/pdf/10.1016/j.febslet.2006.02.027

13. van Ry PM, Minogue P, Hodges BL, Burkin DJ. Laminin–111 improves muscle repair in a mouse model of merosin-deficient congenital muscular dystrophy. Hum Mol Genet [Internet]. Oxford University Press; 2014 [cited 2016 Sep 6];23:383–96. Available from: http://www.hmg.oxfordjournals.org/cgi/doi/10.1093/hmg/ddt428

14. Shultz LD, Schweitzer PA, Christianson SW, Gott B, Schweitzer IB, Tennent B, et al. Multiple defects in innate and adaptive immunologic function in NOD/LtSz-scid mice. J Immunol [Internet]. 1995 [cited 2019 Apr 7];154:180–91. Available from: http://www.jimmunol.org/content/154/1/180

15. Welser J V, Rooney JE, Cohen NC, Gurpur PB, Singer CA, Evans RA, et al. Myotendinous junction defects and reduced force transmission in mice that lack α7 integrin and utrophin. Am J Pathol [Internet]. 2009 [cited 2019 Jul 11];175:1545–54. Available from: https://www.ncbi.nlm.nih.gov/pmc/articles/PMC2751551/pdf/JPATH175001545.pdf

16. Barraza-Flores P, Fontelonga TM, Wuebbles RD, Hermann HJ, Nunes AM, Kornegay JN, et al. Laminin–111 protein therapy enhances muscle regeneration and repair in the GRMD dog model of Duchenne Muscular Dystrophy. Hum Mol Genet [Internet]. 2019 [cited 2019 Jul 11]; Available from: https://academic.oup.com/hmg/advance-article-abstract/doi/10.1093/hmg/ddz086/5479258

17. Wosczyna MN, Rando TA. A Muscle Stem Cell Support Group: Coordinated Cellular Responses in Muscle Regeneration. Dev Cell. 2018;46:135–43.

18. Kuang W, Xu H, Vilquin JT, Engvall E. Activation of the lama2 gene in muscle regeneration: abortive regeneration in laminin alpha2-deficiency. Lab Invest [Internet]. 1999 [cited 2019 Jul 17];79:1601–13. Available from: http://www.ncbi.nlm.nih.gov/pubmed/10616210

19. Yurchenco PD, McKee KK, Reinhard JR, Rüegg MA. Laminin-deficient muscular dystrophy: Molecular pathogenesis and structural repair strategies [Internet]. Matrix Biol. 2018 [cited 2019 Feb 4]. p. 174–87. Available from: https://doi.org/10.1016/j.matbio.2017.11.009

20. North KN, Specht LA, Sethi RK, Shapiro F, Beggs AH. Congenital Muscular Dystrophy Associated With Merosin Deficiency The congenital muscular dystrophies are a heterogeneous group of muscle diseases characterized by early-onset weak-ness, hypotonia, delayed motor milestones, and a high inci-dence of severe [Internet]. J Child Neurol. 1996. Available from: https://journals-sagepub-com.unr.idm.oclc.org/doi/pdf/10.1177/088307389601100406

21. Gawlik KI, Li J-Y, Petersén A, Durbeej M. Laminin alpha1 chain improves laminin alpha2 chain deficient peripheral neuropathy. Hum Mol Genet [Internet]. 2006;15:2690–700. Available from: http://www.ncbi.nlm.nih.gov/pubmed/16893907

22. Rooney JE, Gurpur PB, Burkin DJ. Laminin–111 protein therapy prevents muscle disease in the mdx mouse model for Duchenne muscular dystrophy. Proc Natl Acad Sci U S A. United States; 2009. p. 7991–6.

23. Riederer I, Bonomo AC, Mouly V, Savino W. Laminin therapy for the promotion of muscle regeneration. FEBS Lett [Internet]. Federation of European Biochemical Societies; 2015 [cited 2019 Jun 14];589:3449–53. Available from: http://dx.doi.org/10.1016/j.febslet.2015.10.004

24. Shultz LD, Ishikawa F, Greiner DL. Humanized mice in translational biomedical research [Internet]. Nat. Rev. Immunol. 2007 [cited 2019 Apr 10]. p. 118–30. Available from: www.nature.com/reviews/immunol

25. Mice CB-, Greiner DL, Shultz LD, Yates J, Appel MC, Perdrizet G, et al. Improved Engraftment of Human Spleen Cells in NODILtSz-scid/scid Mice as Compared with C.B–1 7-scid/scid Mice. Am J Pathol [Internet]. 1995 [cited 2019 Jul 9];146:888–902. Available from: https://www.ncbi.nlm.nih.gov/pmc/articles/PMC1869266/pdf/amjpathol00052–0110.pdf

26. Prochazka M, Gaskins HR, Shultz LD, Leiter EH. The nonobese diabetic scid mouse: Model for spontaneous thymomagenesis associated with immunodeficiency (severe combined immunodeficiency mutation). Immunology [Internet]. 1992;89:3290–4. Available from: https://www.ncbi.nlm.nih.gov/pmc/articles/PMC48852/pdf/pnas01082–0136.pdf

27. Pegoraro E, Mancias P, Swerdlow SH, Raikow RB, Garcia C, Marks H, et al. Congenital Muscular Dystrophy with Primary Laminin-a2 (Merosin) Deficiency Presenting as Inflammatory Myopathy. Am Neurol Assoc [Internet]. 1996 [cited 2019 May 13];782–91. Available from: https://onlinelibrary-wiley-com.unr.idm.oclc.org/doi/pdf/10.1002/ana.410400515

28. Fontes-Oliveira CC, M. Soares Oliveira B, Körner Z, M. Harandi V, Durbeej M. Effects of metformin on congenital muscular dystrophy type 1A disease progression in mice: a gender impact study. Sci Rep [Internet]. 2018 [cited 2019 Apr 24];8. Available from: www.nature.com/scientificreports/

Figures

Figure 1. Barraza-Flores et al. 2019

Figure 1

The NODScid dyW mouse model of LAMA2-CMD shows downregulated levels of Laminin-α2 protein chain and is immuno deficient. (A) Detection of Laminin-α2 (red) in Tibialis Anterior (TA) sections of wild type, dyW internal control, dyW, and NODScid dyW. Scale bar 100 μm. (B) Relative levels of immunoglobulin in sera of wild-type, NOD Scid, dyW and NODScid dyW (N=9; p-value <0.0001) (C) Fluorescence-activated cell sorting (FACS) gate analysis of hematopoietic cells (CD45+) from sera of wild type and NODScid dyW co-labeled with T-cell marker (CD3ε+) and B-cell marker (CD19+).
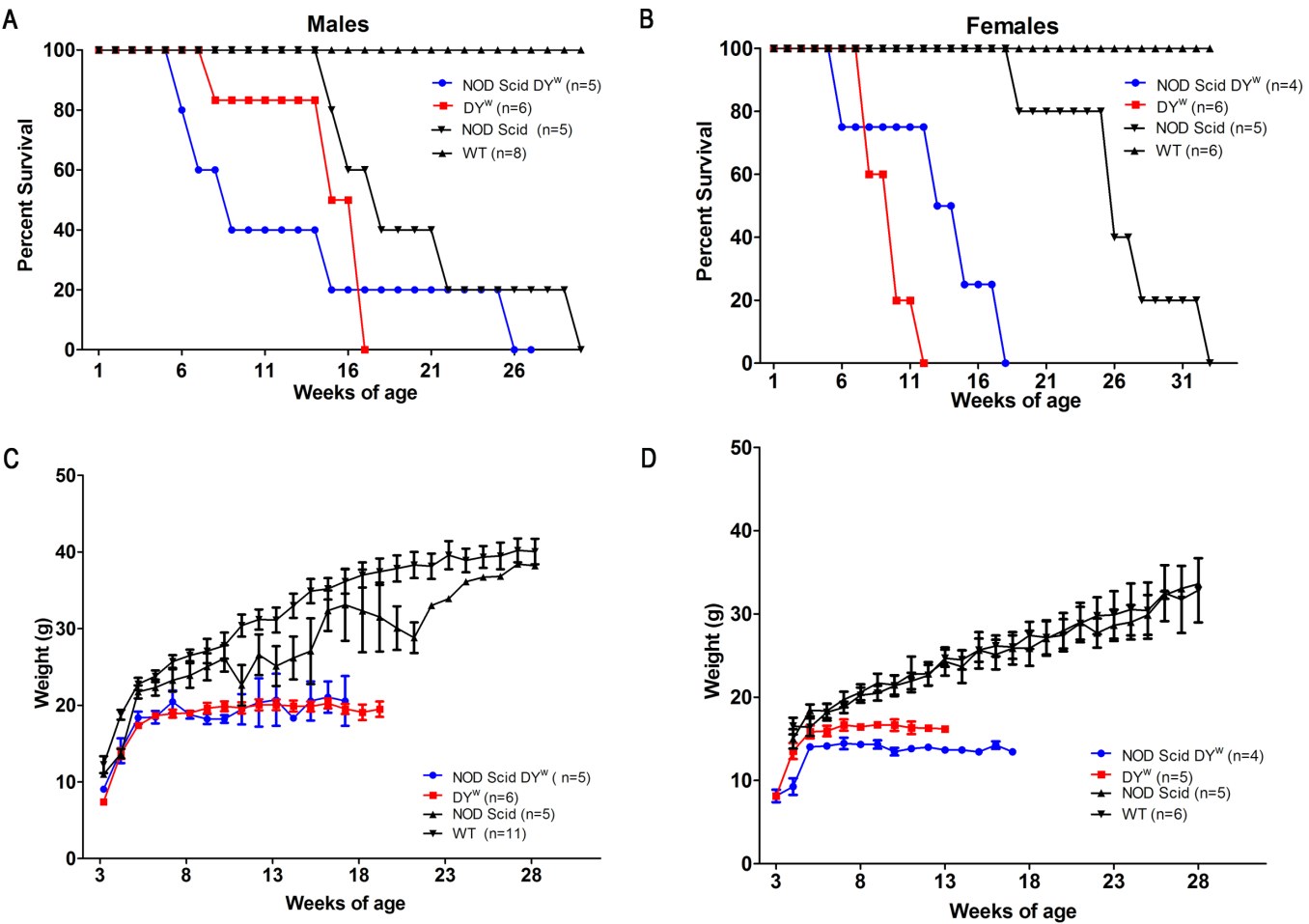
Figure 2. Barraza-Flores et al. 2019

Figure 2

Survival and weight did not change in immuno deficient mouse compared to immuno competent mouse models of LAMA2-CMD. Survival study curves of male (A) and female (B) wild type, NOD Scid, dyW and NODScid dyW. (C) Weekly weights throughout life span of male and female (D) wild type, NOD Scid, dyW and NODScid dyW.
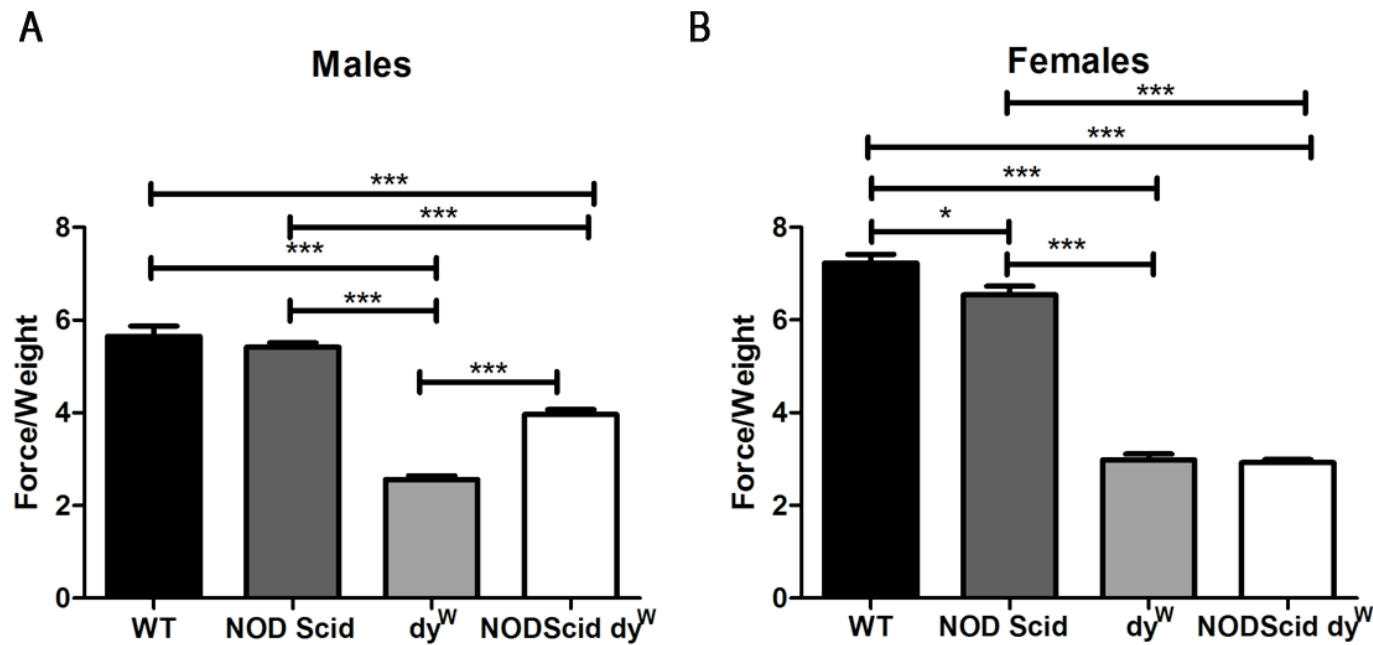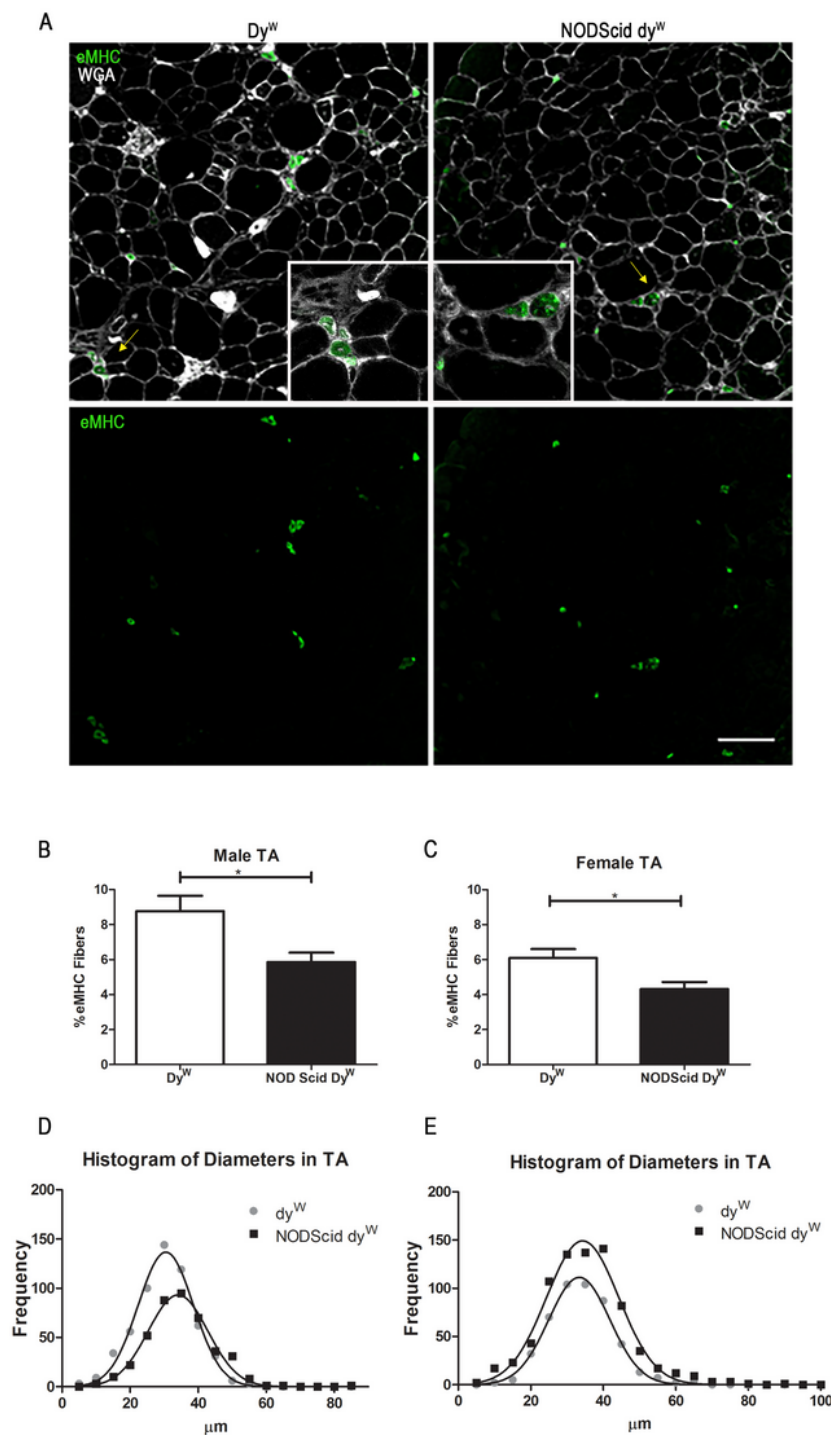
Figure 3. Barraza-Flores et al. 2019

Figure 3

Grip strength is increased in immuno deficient male mice compared to immuno competent LAMA2-CMD mouse models. Normalized force measurements of grip strength in wild type, NOD Scid, dyW and NODScid dyW (A) male (N=4, 5, 7, 6 respectively; p-value <0.0001) and (B) female (N=5; p-value <0.05*, <0.0001***).

Figure 4. Barraza-Flores et al. 2019

Figure 4

Basal regeneration is decreased in immuno deficient compared to immuno competent mouse models of LAMA2-CMD. (A) Detection of embryonic Myosin Heavy Chain (eMHC) in TA sections of dyW and NODScid dyW mice. Quantification of eMHC positive fibers in male (N=7, 5 respectively; p-value of 0.01). Scale bar 100 μm. (B) and female (N=5, 4 respectively; p-value of 0.02). (C) DyW and NODScid dyW mice.

Frequency histogram of minimum Feret's diameters in TA muscle of male (N=4, 5 respectively; p-value <0.0001) (D) and female (N=5; p-value <0.0001) (E) dyW and NODScid dyW mice.
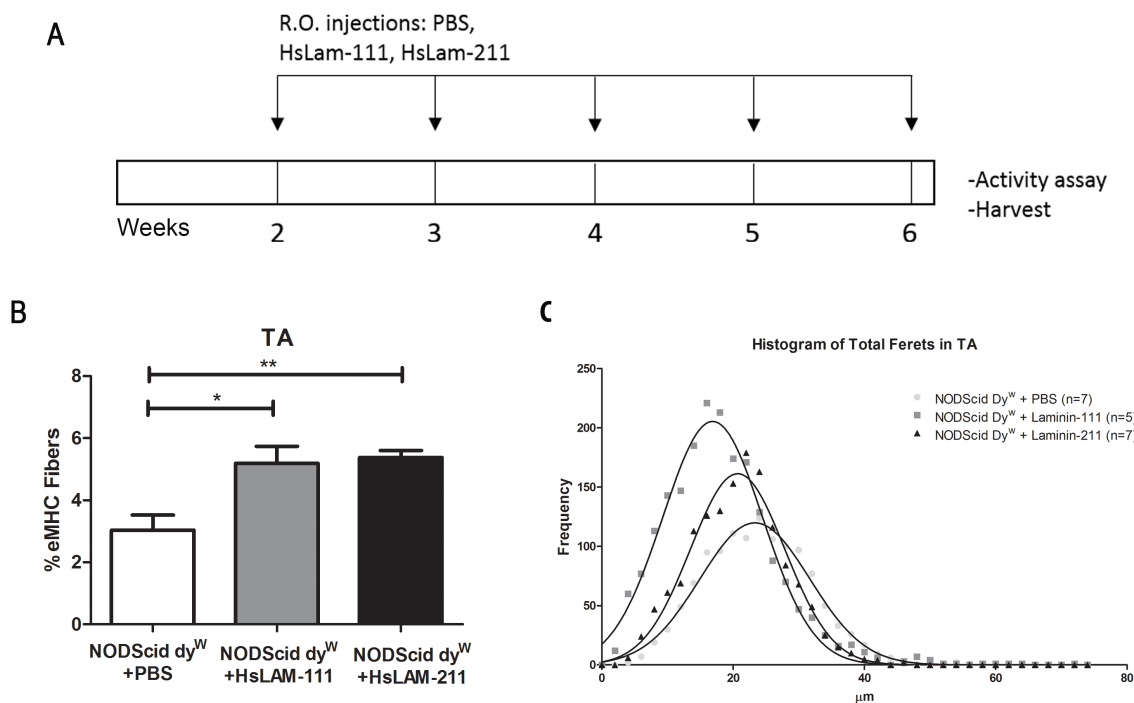
Figure 5. Barraza-Flores et al. 2019

Figure 5

Treatment with human recombinant Laminin-111 (HsLAM-111) and human recombinant Laminin-211 (HsLAM-211) increases regeneration in mouse model of LAMA2-CMD. (A) NODScid dyW mice were treated with weekly retro orbital injections of 1mg/kg HsLAM-111, HsLAM-211 or PBS from 2 weeks to 6 weeks of age. (B) Quantification of eMHC positive fibers in PBS, HsLAM-111 and HsLAM-211 treated NODScid dyW (N=7,5,6 respectively; p-value <0.05*, 0.0049**). (C) Frequency histogram of minimum Feret's diameters in TA muscle of PBS, HsLAM-111 and HsLAM-211 treated NODScid dyW (N=7,5,7 respectively; p-value < 0.0001).
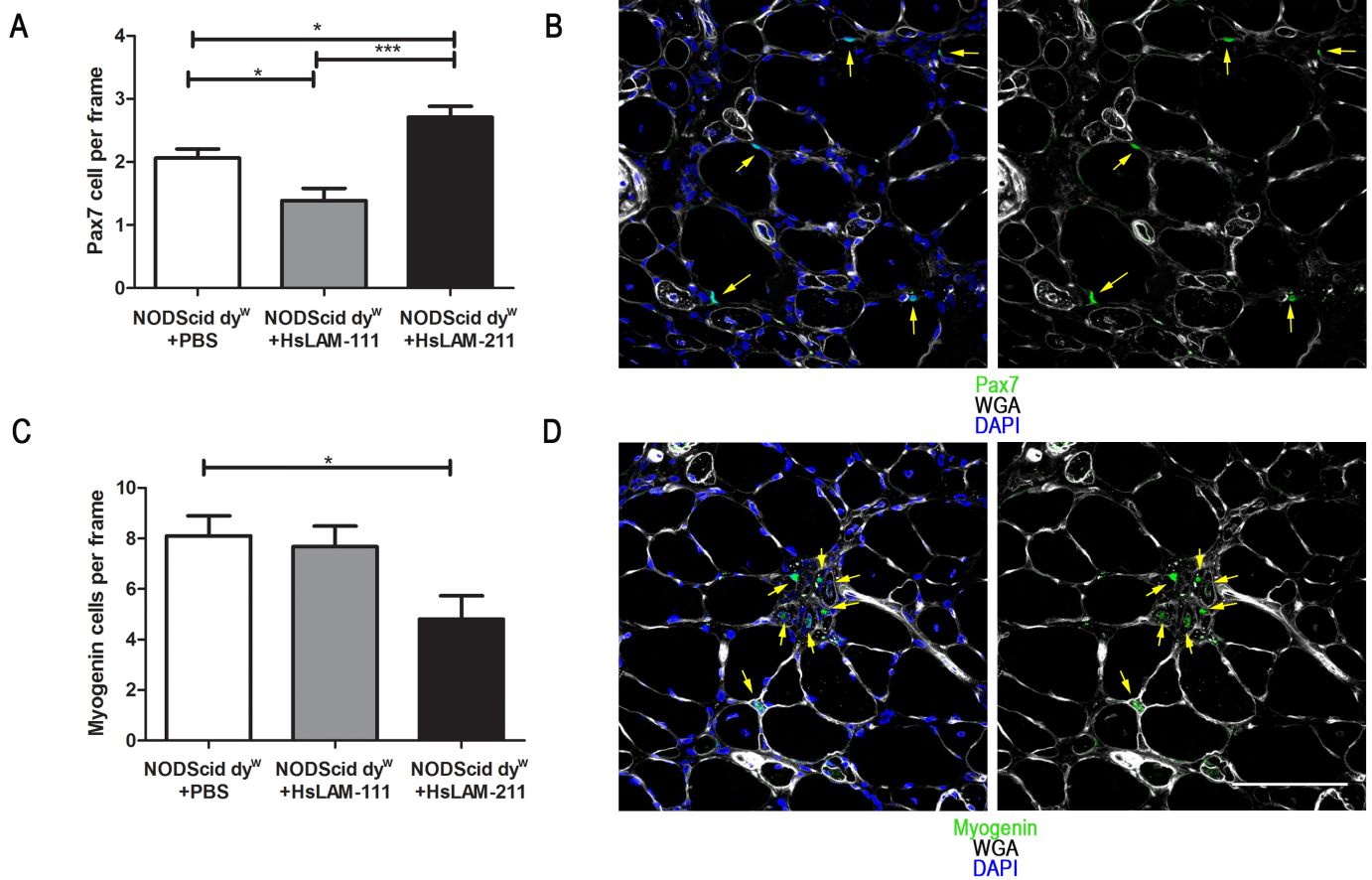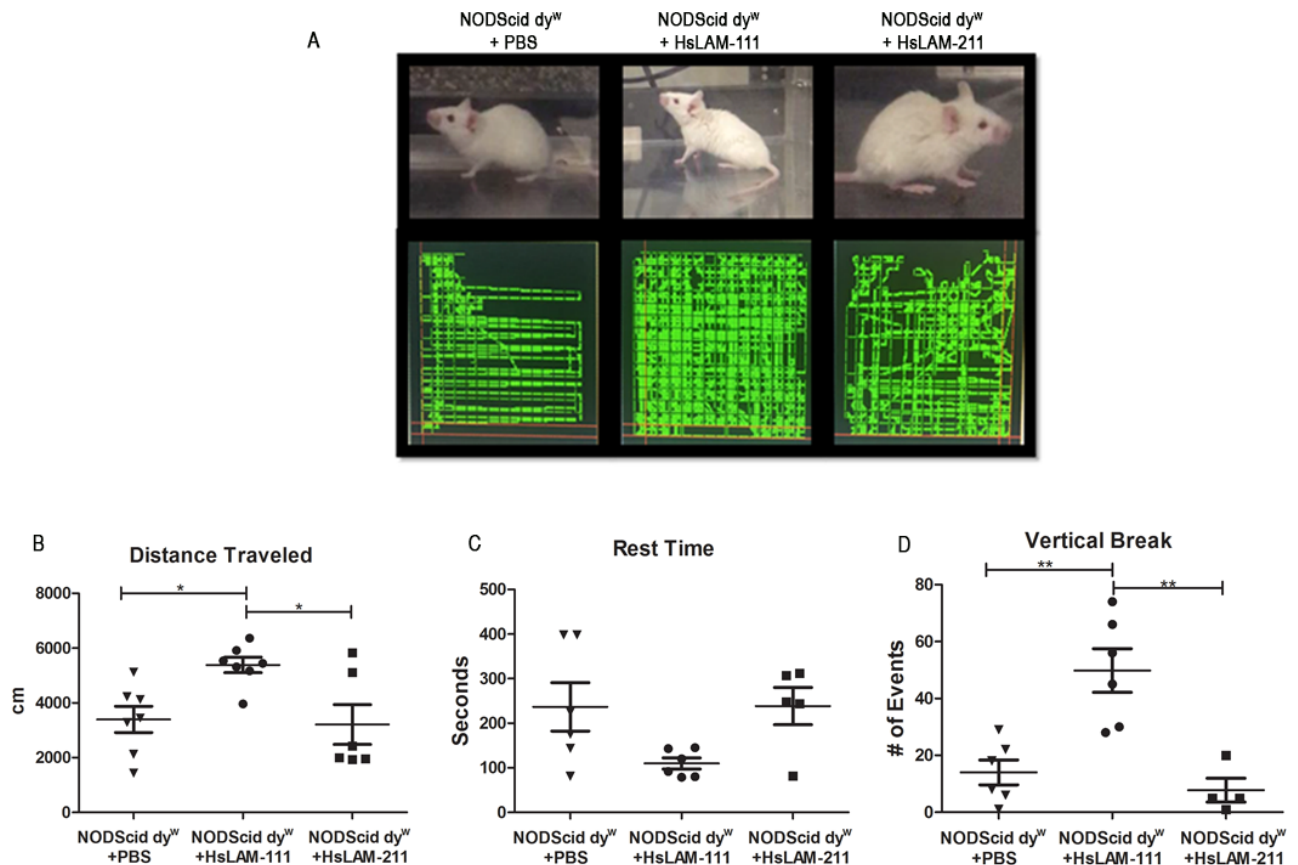
Figure 6. Barraza-Flores et al. 2019

Figure 6

Treatment with HsLAM-111 and HsLAM-211 differentially affects satellite cells and myoblasts in skeletal muscle of LAMA2-CMD. (A) Quantification of Pax-7 positive satellite cells per frame in TA muscle sections of PBS, HsLAM-111 and HsLAM-211 treated NODScid dyW (N=8, 6, 6 respectively; p-value < 0.05* <0.0001***). Scale bar 100 µm. (B) Detection of Pax7-positive cells adjacent to fibers in TA sections of NODScid dyW mice. (C) Quantification of myogenin-positive myoblasts per frame in TA muscle sections of PBS, HsLAM-111 and HsLAM-211 treated NODScid dyW (N=7; p-value of 0.019). (D) Detection of myogenin-positive cells located interstitially in TA sections of NODScid dyW mice.

Figure 7. Barraza-Flores et al. 2019

Figure 7

Treatment with HsLAM-111 improved mouse activity in LAMA2-CMD mouse model. (A) PBS, HsLAM-111 and HsLAM-211 treated NODScid dyW mice pictures and trajectory detected using computer-controlled activity assay. Quantification of distance traveled (B), resting time (C) and vertical breaks (D) in PBS, HsLAM-111 and HsLAM-211 treated NODScid dyW (N=7,7,6 respectively; p-value <0.05*, <0.005**).

Supplementary Files

This is a list of supplementary files associated with this preprint. Click to download.

- BarrazaFloresetal.supplementalfigures.docx